doi:10.3788/gzxb20174606.0612003

对复杂自由曲面的纹理重建方法

刘星明[1],蔡铁[1],李阿蒙[2],王辉静[1],闫立军[1]
(1 深圳信息职业技术学院 计算机学院 智能彩色成型技术工程实验室,广东 深圳 518172)
(2 深圳大学 光电工程学院 教育部光电器件与系统重点实验室,广东 深圳 518070)

摘　要:提出一种基于马尔科夫优化策略复杂自由曲面的纹理重建方法,该方法利用实验室研制的三维数字化设备对目标物体的深度数据和纹理数据进行采集,将局部采集的深度像数据匹配到全局坐标系下,建立物体的几何模型;然后通过坐标变换,把采集的纹理照片映射到重建的几何模型表面,并进行曲面纹理融合处理,实现自由曲面的纹理重建.该方法对物体的形貌没要求,能实现结构复杂的自由曲面的纹理重建,得到高保真质量的真实感模型.采用该算法对几种不同的实物进行数据采集和真实感三维重建,实验结果验证了算法的可靠性和有效性.

关键词:机器视觉;三维测量;条纹投影;纹理融合;相机标定
中图分类号:TN391　　**文献标识码**:A　　**文章编号**:1004-4213(2017)06-0612003-10

Texture Reconstruction Method for Complex Free-form Shapes

LIU Xing-ming[1], CAI Tie[1], LI A-meng[2], WANG Hui-jing[1], YAN Li-jun[1]
(1 *Intelligent Color Molding Technology of Engineering Laboratory, School of Computer Science, Shenzhen Institute of Information and Technology, Shenzhen, Guangdong* 518172, *China*)
(2 *College of Optoelectronic Engineering, Key Laboratory of Optoelectronics Device and system, Education Ministry of China, Shenzhen University, Shenzhen, Guangdong* 518060, *China*)

Abstract: A texture reconstruction method based on Markov random fields optimization was proposed to reconstruct the complex free-form shapes. The method used a three-dimensional digital device developed by laboratory to capture the range data and the texture images, and registered the local capture range data into global coordination system to establish the surface of the object. To build a realistic textured model, the captured texture images were mapped to the reconstructed surface by coordinate transformation, and a texture fusion processing was followed. The proposed method does not impose any constraints on the topology of the surface, and a realistic textured model of the free-form surface can be achieved. The data collection and realistic three-dimensional reconstruction of material object were experimented by the proposed method, the results show the reliability and effectiveness of the proposed method.

Key words: Machine vision; Optical measurement; Stripe projection; Texture blending; Camera calibration
OCIS Codes: 120.1880;100.2650;100.6890

0　Introduction

The recovery and representation of geometry, topology and natural appearance of 3D objects in the

Foundation item: The Natural Science Foundation of Guangdong Province (No. 2015A030310511), Shenzhen Science and Technology Project (Nos. JCYJ20150417094158019, JCYJ20150417094158026).

First author: LIU Xing-ming (1982—), male, lecturer, Ph. D. degree, mainly focuses on computer vision, 3-D measurement technology. Email: xlium@126.com
Contact author: CAI Tie (1977-), male, professor, Ph. D degree, mainly focuses on information processing. Email: Cait@sziit.edu.cn

Received: Jan. 16, 2017; **Accepted**: Mar. 20, 2017

real scene is one of the most challenging problems in the fields of optical engineering, computer vision and computer graphics. Generation of a high-quality photorealistic model of 3D objects in real world plays an increasingly significant role in the garment design, cultural heritage, and virtual reality in addition to traditional applications in the industry inspection and reverse engineering[1-3]. In past decade, on one hand, most of research efforts have been made on the high-precision shape recovery of 3D objects with the help of laser scanner or optical digitizer[4-6], focusing on the accuracy improvement of reconstructed models of 3D objects. On the other hand, the issue of recovery of natural appearance of 3D objects has not been addressed sufficiently in the field of optics[3,7-10], likely due to the cross-interdisciplinary obstacles. Nevertheless, this issue is becoming more and more important to create photorealistic models of 3D objects in the real scene as required in cultural heritage.

To build high-quality 3D objects of the real world, a specific designed 3D laser scanner or an optical digitizer is usually employed to acquire range images from different viewpoints. Nowadays, The improvements of hardware and software of digital photography makes it possible to acquire very dense sampling of both geometric and optical surface properties of real objects. Modern 3D scanners can sample a surface with a sampling rate as small as 0.25mm and produce very detailed 3D models (composed of millions of triangles) in a very short time with the support of software tools[10-11]. For all but the simplest objects, the captured range images must be acquired from the different views to cover the whole object′ surface. And the captured range images must be aligned, or registered, into a common coordination and then integrated into a single 3D model. The systems registration may be performed by accurate tracking, such as attached the scanner on the scanner system to track its position and orientation with a high degree of accuracy. Also, many scanner systems rely on interactive alignment by human operator to pick the corresponding points to compute a rigid transformation that aligns the points. After the registration of multiple range images the registered range images can thus be integrated to create a complete and non-redundant 3D geometric model. However, due to the lack of the natural appearance of the surface, which has lot limitations in the application of virtual reality and cultural heritage et al.

In the last decade, the vision community has made substantial progress in addressing the problem of recovering natural appearance of 3D textured model. The most of researches using kinds of blending methods between fragments, with a weighting average of fragments over the whole mesh, like works[10,12-13]. Others employ a mosaic procedure to deal with visual artifacts along the fragments, and feather seams to remove the visual artifact on the model surface[14-15]. These strategies are based on intension blending, and its resampling procedure of texture blending are not well suited for objects with complex topology structure, like parametrization of complex topology object for mapping the captured texture images onto the surface. Therefore, a general texture blending method should be able to process free-form target in order to be useful in application involving the photorealistic reconstruction of real-world objects. This paper proposed a general and novel solution to the problem of reconstruction of textured model. In our presented approach, the geometric model and its surface texture of 3D modes are recovered, which have an important applications in the area such as object inspection and heritage conservation. The proposed algorithms avoid the resampling procedure and ensure the high-resolution of the produced texture as well as the original input views, even in the situation like with some errors in the stages of reconstruction.

1 Optical digitizer for creating a photorealistic model

The first step for reconstructing a photorealistic model of real-life object is to acquire range images and associated color images, which can be done by use of a 3D optical digitizer, similar work also done by D. Towers and Zhang′s group[16]. Here we describe a dedicated optical digitizer recently developed in our laboratory for this purpose. The principle of our dedicated optical digitizer is based on the Fringe Projection Profilometry (FPP)[17]. The layout of a modified scheme of the fringe projection profilometry (m-FPP) is schematically shown in Fig. 1 where the Digital Micro-mirror Device (DMD) projector providing structural illuminations works with a Black-and-White (B/W) camera (RC camera), and another digital color camera Texture Camera (TC), are attached to this FPP sensor head and used to capture associated texture images of the 3D object. The DMD projector and RC camera together with color camera TC result in a m-FPP and a dedicated optical digitizer for creating photorealistic models of 3D objects in a real scene.

When the system works, the DMD projector projects a pattern of masked light onto the object to be scanned, and using the RC camera to capture the reflected light from the object. Meantime, the surface attribute properties is captured by the TC camera, due to the capture system (TC camera attached on the scan system), the relationship between the RC camera and TC camera can be determined through calibration (the camera calibration will be discussed in the Section 2). And if the camera parameters (internal parameters and external parameters) are known, followed with the triangulation theory (Fig. 1), the array of depth values can be calculated.

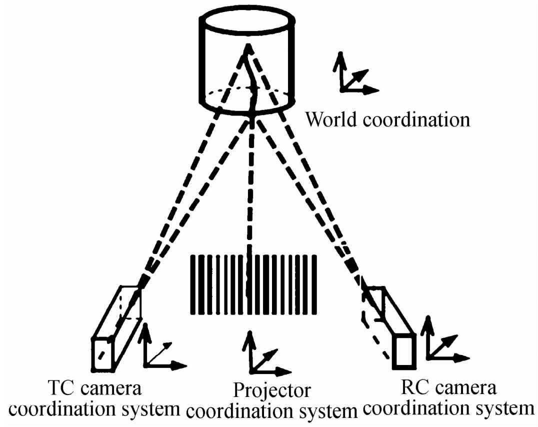

Fig. 1 Layout of the dedicated acquisition system

The scan system provides clouds of 3D points, and additional information also provided, such as the normal of space points, which can be calculated by cross products of neighbor vectors, and the triangular mesh, topology of scanned object also can be calculated from the cloud of points.

In our scan system, the TC camera in m-FPP based optical digitizer is fixed with respect to the RC camera and the DMD projector. Then the rigid transformation between the RC camera and the TC camera can be determined accurately by calibration, which is advantageous to reduce the incoherence texture on the texture mapping.

2 Sensor calibration and pose estimation of texture camera

2.1 Sensor calibrations

Calibration is the technique to estimate all system parameters (the internal parameters and external parameters of the camera are (K, R, t)). For simplicity, we introduce short notations $(K_{c/p}, k_{c/p})$ and $(R_{c/p/s}, t_{c/p/s}) \rightarrow \Theta_{c/p/s}$, (subscribe means in the different coordination system, e. g. $K_{c/p}$ represents the internal parameters of the RC camera and the DMD projector) . In our system, a convenient calibration for the m-FPP is to use a planar reference target on which white dots of known positions (also referred to as benchmarks) are printed. When calibration performed, the target will be placed in different positions and orientations (poses) within the scheme measurement volume. If the world coordinate system is placed on the sensor, it means the calibration target changes its poses with respect to the sensor times. For each pose, first an image of the target is acquired under uniform illumination and the image points of benchmarks can be located. Then the fringe patterns are sequentially projected on the calibration target and then captured by the camera. Thereby the absolute phase maps can be calculated. And the homologous point can be determined by using the constraint. Now the camera and projector can be calibrated with Zhang′s method respectively, which will provide a series of parameters: $\theta_c, \theta_p, \Theta_c^i, \Theta_P^i, i=1, \cdots, N$. To get the globally optimal estimation of the parameters, we have defined the following cost function in Ref. [18].

$$\text{cost}(\tau) = \sum_{i=1}^{N}\sum_{j=1}^{M}\left(\| \hat{m}_c^{ij} - m_c^{ij}(\theta_c, \Theta_c^i; X_w^j) \|^2 + \| \hat{m}_p^{ij} - m_p^{ij}(\theta_p, \Theta_s, \Theta_c^i; X_w^j) \|^2 \right) \tag{1}$$

where $\tau = \{\theta_c, \theta_p, \Theta_s, \Theta_c^i, X_w^j\}$ is the parameters vector to be optimized, superscript i denotes the i^{th} pose and j the j^{th} benchmark, m_c^{ij} is the reprojection image coordinate of the camera, m_p^{ij} of the projector. Minimization of Eq. (1) is a nonlinear least square problem, which can be solved with Levenberg-Maquardt (LM) method.

2.2 Pose estimation of TC

To texture map, we further place the sensor coordinate system of optical digitizer on the B/W camera

(RC) so that the viewpoint of the range sensor is transformed to that of the RC. In this case, the color image must be transformed to the RC of the sensor coordinate system. To do this, we also need to transform the range image from the TC coordinate system to that of the RC. In this way, the correspondence between the range images (in the RC coordinate system) and associated color images can be established precisely.

In m-FPP, the natural appearance (color image) of real object can be captured by digital color camera (TC) with controlled illumination condition. Since the photos taken follow the law of the perspective, if we know the camera parameters we can determine if (and where) a point on the object surface is mapped within the overlapped regions or inside the image boundaries. An efficient way to compute those pixel-to-surface correspondences is by rendering the 3D model (range images) with the same projection parameters of the given photo. In this way, the range image (depth map) can be used to discriminate whether or not a point on the surface that projects inside the color image is visible or whether it is occluded by other geometry. In this way, it is possible to safely assign a pixel color, taken from that photo, to a point onto the surface. Digital color camera and B/W camera are also fixed with respect to each other so that the rigid transformation between digital color camera and B/W camera can also be deduced.

The m-FPP configuration utilizes one B/W camera working together with a projector for range image acquisition in which the absolute phase map is merely used for the establishment of point correspondence. Additional digital color camera is used for color image acquisition and the transformation between the RC coordinate system and that of the TC can be accurately determined from calibration using the calibration of Zhang′s method[18]. In other words, the RC camera and TC camera are fixed on the system, so the relationships between the coordination systems can be accomplished through calibration, then to project the range image onto the TC camera to get the color information of every 3D data.

2.3 Registration and integration of color-textured range images

Once the optical digitizer based on m-FPP is calibrated, the range images associated with the surface color images of the scene can be acquired. And with the help of TC camera pose (details discussed in the previous section), the color images can be back-projected onto the corresponding surface, got the texture patch. However, due to the limitation of the san view, the scan view should be adjusted several times to get the whole range images associate color images to cover the whole surface, or put object on a turntable to capture all source data. Usually, this procedure would take some times according to the size and the topology complex of the objects, sometimes, even take several days to acquire a big-size heritage, like the Michelangelo′s Florentine Pieta[19]. In the particular system scan, Suppose the kth view, its range images and the corresponding color images are $\{X_{\mathrm{RC}k}(x,y,z), k=1,2,\cdots,K\}$ and $\{I_k(R,G,B), k=1,2,\cdots,K\}$, respectively.

In order to get a complete model, the individual range images must be aligned, or registered into a common world coordination system so that they can be integrated into a single 3D model. There many successful registration methods in the past decade are proposed by the researchers, like using coordinate measurement machine to track the scan system′s position and orientation with a high degree of accuracy, or using a turn-table to get an initial registration, following with an optimization algorithm to get a high accuracy transformation. In our experiment, the interactive alignment strategy is adapted: identifying several corresponding points on the range images to compute a rigid transformation that align the range images, and followed with the Iterative Closest Point (ICP) algorithm[20], which iterative the process until some convergence criterion is satisfy to get the best rigid transformation and reduce the distance among scans. It is worth noting that, the process may converge to a local minimum, pick the right initial alignment is an important factor to get a global minimum.

The color images can be used to facilitate the alignment in our scan system because of the TC camera is fixed on the scan. In other words, which means the relative position and orientation of the color images and range images are known, then the texture information can be used in the initial alignment phase and finally improve the optimization procedure. That has the advantages, especially when there have few geometric features, the color image of surface can greatly help to improve the accuracy of the algorithm.

Align the different coordination system into a common system, and merge the aligned multiple scans into a unified surface representation, reconstruct the geometry and topology of the scanned object, this procedure can be mathematically described as follows

$$\{X_{uk}(x,y,z;R,G,B)\}\to M\{V_i(x,y,z;R,G,B)\} \quad i=1,\cdots,N \tag{2}$$

where M stands for mesh model that is consisted of a complete and non-redundant point cloud and connectivity representing the topology of the model. The vertices V_i of point cloud comes from data set of range images, and each vertex is associated with a given color (RGB) coming from associated color images.

3 Photorealistic reconstruction of 3D objects

Due to the variation of environmental lighting and inaccuracy of geometric model reconstruction, the incoherence exists within the overlapped region and leads to unnatural visual artifacts. Therefore, a texture blending method of 3D model should be applied to remove the visual artifacts within the overlapped regions. Unlike those methods reported in previous literatures, in this paper, a more general framework for texture stitching approach is taken by using an energy of Markov Random Field (MRF) optimization strategy.

The MRF strategy consist two terms, the first term measure the quality of the "Best" view, like the most orthogonal color images to map onto the surface with better quality, if the color images is not fit to map onto the surface, its energy is set to large, like set to ∞. The second term measures the incoherence of the adjacent texture patches. Therefore, we propose to get the minimum value sum of the two term, measure the quality of the texture map, and this mosaic $\boldsymbol{M}$ mathematically described as

$$\mathrm{Min}\left\{\sum_{i=1}^{N}\boldsymbol{E}_{\mathrm{data}}(f_{\Delta_i}{}^{m_i})+\lambda\sum_{i=1}^{N}\boldsymbol{E}_{\mathrm{Smooth}}(f_{\Delta_i}{}^{m_i},f_{\Delta_j}{}^{m_j})\right\} \tag{3}$$

where, $f_{\Delta_i}^{m_i}$ is the triangle Δ_i associate with the m_i view(m_i-th image), and m_i belong to one of the input views, $\boldsymbol{E}_{\mathrm{data}}$ is smaller for the orthogonal view. While the second term measure the discontinuity of the adjacent boundaries. Let's assume theF_{ij} is the adjacent boundaries of different triangles, this term can be described as

$$E_{\mathrm{Smooth}}(f_{\Delta_i}{}^{m_i},f_{\Delta_j}{}^{m}_{j})=\int_{F_{ij}} d\left(\prod_{m_i}(X),\prod_{m_j}(X)\right)\mathrm{d}X \tag{4}$$

where $\prod_{m_i}$ is the projector matrix for the m_i-th image, $d(\cdot)$ is the Euclidean distance in the color space (for example, Euclidean distance in RGB color space can be used for that purpose), and λ is a scale factor, that used to balance the two terms in the optimization procedure. Compared to the works that choosing the "Best" view to map onto the surface, our optimization strategy is based on the quality of the views and the incoherence of the texture of the surface, which is more suitable for mapping and a better result can be produced. In our actual experiments, the scale is set to a fix value: $\lambda=1$, which means the two terms have been considered and have the same factors for mapping. Here, when $m_i=m_j$, which means triangle Δ_i and triangle Δ_j texturing from the same image, then equals zero (texturing from the same image does not cause artifacts). In our approach, the MRF is mesh-based, its nodes correspond to mesh facets, and node interactions are defined by facets of adjacency. The remaining intensity discontinuities require further processing, therefore, we propose an approach to remove the residue intensity discontinuities in order to reduce the algorithm complexity of seam leveling.

3.1 Removal of residue seams and other incoherence

In the section, a method for removing the residue seams and other incoherence along with the boundaries is presented, resulting a photorealistic textured model. To do this, we first detected the boundaries of the mesh model between texture patches. A boundary is defined when vertices of underlying triangle are textured from different views (e.g. texturing from two or three images). Removing the seams or artefacts across the boundary is a natural way that mapping the multiple images of a single object onto the reconstructed model. As we just discussed, only used the MRF strategy is not enough for producing a high quality textured 3D model. In this paper, a more sophisticated image contents is considered, which a combination of the image colors and its gradients

$$E_{\mathrm{boundary}}=\sum_{i=1}^{n}\alpha\parallel I_1(s_i)-I_2(s_i)\parallel+(1-\alpha)\parallel G_1(s_i)-G_2(s_i)\parallel \tag{5}$$

where, α the scale parameter, used to proper balance between color and its gradient. $I_1(s_i)$ and $I_2(s_i)$ are the colors of image I_1 and I_2 at point s_i, $G_1(s_i)$ and $G_2(s_i)$ are the color gradients in the captured texture images. Note, Eq. (5) is usually used in the 2D image blending. However, in this paper, we extended the image blending method on the 3D surface to remove the artifacts on the geometric surface. This texture blending method used in the 3D domain is more complicated than in the texture images areas.

3.2 Improvement of details

The texture information on the surface is critical since we do not want to introduce any discontinuity or artifacts on the 3D model surface. However, a potential problem may be arose for in-sufficient accuracy in the following phases, due to: 1) the use of a simplified geometric model that does not take into all of the all the possible factors, likes the noise influence in the capturing of range images; 2) errors of the all stages such as the registration of the range images that from the local coordination into a common system, the integration for removing the redundancy in the overlaps. Therefore, the errors of all the reconstruction phases may bring artifacts to the final textured model, especially when the reconstructed model with pictorial detail, Ghost effects are more easily perceivable if the surface detail contains such as thin lines or abrupt changes of the color information.

In order to enhance the details for visualization , a local registration is taken to adjust the errors of object reconstruction and enhance the details of the final experimental results (note: compared to the registration phases, the local registration only works on the border). This is a similar work in the area of blending the 2D images together. They provide a solution to remove the ghosting effects by aligning the points of the corresponding patches on different images with cross-correlation. This work is extended to the 3D surface reconstruction for producing a high-quality model. The local registration start from the model surface and restrict texture blending to the associated border of the patches, which by mapping the point of the surface to the corresponding captured images and maximizing the cross-correlation between these corresponding texture sections. For our purpose, each border we simple compute a local registration to alignment the errors introduced from the several of the reconstruction phases.

4 Experimental results and discussion

To evaluate the effectiveness of our proposed approach, in this section, the method to generate a photorealistic model with seamless texture montage is validated in a series of experiments under a large variety of conditions. All 3D models have been produce with optical digitizer, which the captured surface is not topologically clean, e. g, contains some outliers of space points which need to be handled before the reconstruction. The database is made of sets of real range images of complex objects representing a Buddha, porcelain, pottery, and jade ware. Experimental results for porcelain, jade ware are stated in this paper. These two reconstruction objects are common in our usual life and contains holes, which represent a key challenge for any reconstruction algorithm, especially with a high-quality texture details on the reconstruction surface.

Fig. 2 Layout of the m-FPP

The experimental setup used in this experiment is a prototypes of 3D optical digitizer developed in our laboratory, as shown in Fig. 2. This dedicated optical digitizer is based on a m-FPP, which is composed of a digital color camera (DFK 41AF02 with 1 394 interface and 1 280×960 resolution), a B/W camera (DMK 41BF02 with 1 394 interface and 1 280×960 resolution), and a DMD projector (LG HX300G-JE with 1 024×768) as basic units. This 3D sensor system was calibrated using the technique described in Section 3, which in order to get accurate cameras and structural parameters as described in Section 3, Fig. 3(a) shows the targets for calibration, several poses of the target were used to calibrate the parameters of the system. The poses of the cameras are shown in Fig. 3(b), the number represents the different capture views. The calibration step minimizes the total re-projection error over all the calibration parameters (intrinsic: focal, principle point, distortion coefficients, and extrinsic parameters), and the optimization is done by iterative gradient descent with an explicit computation of the Jacobian matrix.

Once this was done, the m-FPP sensor can be used to acquire the range images and associated texture images, and the mapping relationship between the mesh model and associated texture images has been established in a precise way after the calibration. Therefore it is possible to back project the associated texture images onto the mesh model (rendering in terms of computer graphics) accurately to produce textured fragments.

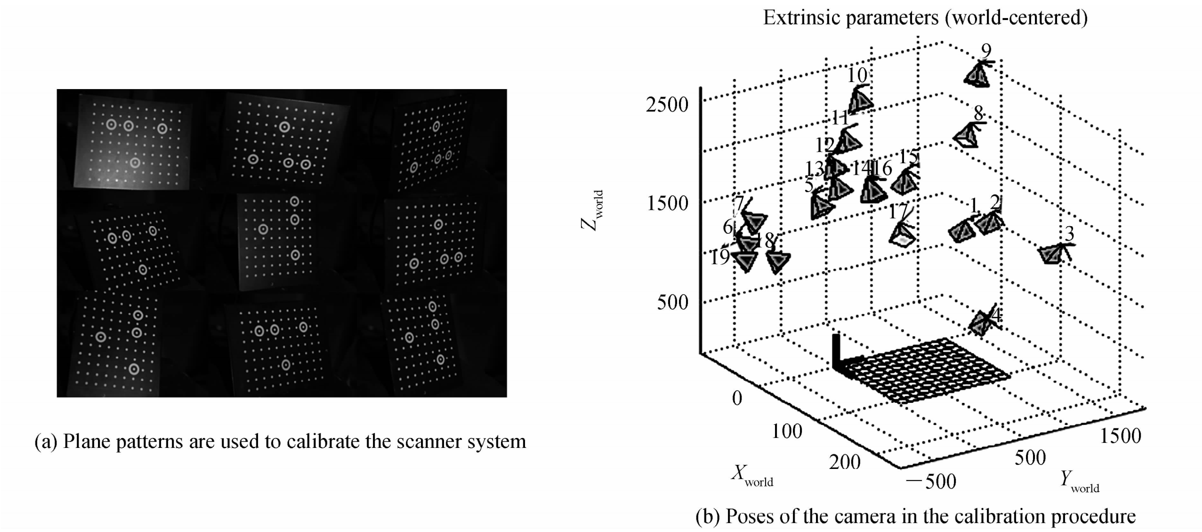

Fig. 3 System calibration results

In order to demonstrate the algorithm, a Buddha which representative of a culture relic is used for reconstruction. The Buddha was placed on a holder stage, and the range images of the vase and associated color images were acquired from 12 views by moving the m-FPP sensor around the subject. Then the multi-view colored range images were registered and integrated to form a complete and colored 3D mesh model using the method discussed in Section 3.3. The whole size of the reconstructed mesh model was 18M, and it was simplified to facilitate further processing. The relationship between the geometric surface and the captured images are accurately calibrated. Once the relationships is determined, the texture map in this case can be obtained by s simple stacking of the initial views (as shown in Fig. 4). Usually, to make the mapping more compact, the unused parts of the texture are removed and the used parts are packed on a plane.

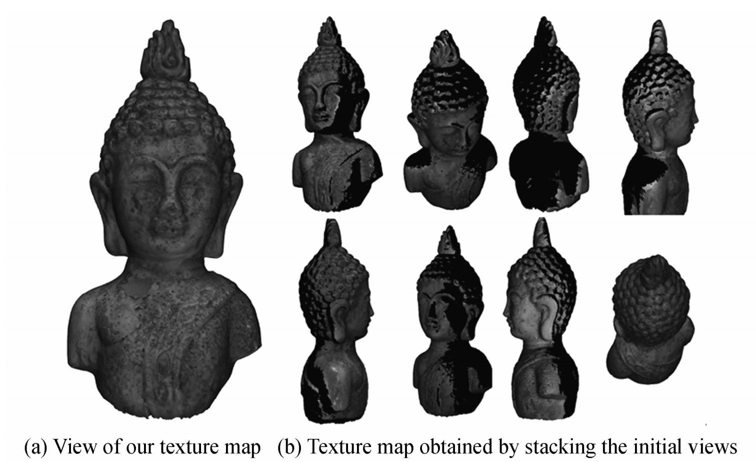

Fig. 4 Texture maps created with the proposed method employ a texture mapping defined by projections operators

For our purpose, this paper extended the MRF algorithm on the 3D geometric surface which is more complicated compared with in the planer image texture synthesis. In our case, the MRF is mesh-based, which correspond to mesh patches. For our purpose, using the MRF algorithm to mosaic texture to the geometric surface, which converges to a lowest value of energy with the smallest time. As shown in Fig. 5. The optimized mosaics can obtained the high-quality texture details compared with the "Best view" algorithm which preference to the less oblique for map.

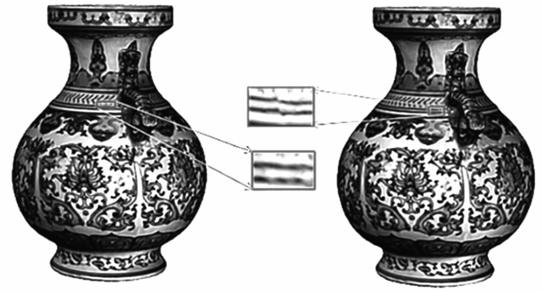

(a) "Best view" algorithm　(b) Proposed algorithm

Fig. 5　Experimental results

Fig. 6 shows the textured mesh for the pottery, the 3D model is composed by 8964 triangles, with a mapped photographic data set of 6 images 1 280×960. Fig. 7 shows the textured mesh for the jade, the 3D model is composed by 3 862 triangles, with a mapped photographic data set of 6 images 1 280×960. All the range images data and the associate texture images data are captured with our own developed digitizer, and the multi-view partial range images were then registered and integrated into a complete model. Next, the captured texture images have been aligned to the 3D geometry by using our calibration procedure. The calibration algorithm is able to compute the intrinsic and extrinsic camera parameters by following the using a standard approach of capturing several planar targets. Once these prerequisite conditions are satisfied, we are able to generate a high quality and high resolution photorealistic 3D model of real object with our proposed approach.

(a) Point-based geometry (b) Solid-based geometry (c) One viewpoint (d) Another viewpoint

Fig. 6　Textured mesh of pottery

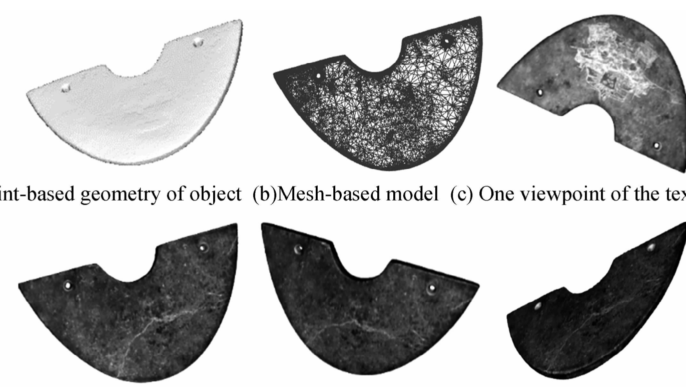

(a) Point-based geometry of object (b)Mesh-based model (c) One viewpoint of the textured model

(d) Viewpoint of results from front (e) Viewpoint of results from the side (f) Viewpoint of results from another side

Fig. 7　Textured mesh of jade-ware

A sequence of geometric model of the porcelain were used to show the capability of our proposed method. The highest resolution mesh-based model has 20 000 triangles and the conventional decimation was used to generate with 8 000 and 3 000 triangles. The computation time for several texture image resolutions is shown in Table 1, and the timings were taken on a Intel 3.4 GHz Core processor.

Table 1 Algorithm performance of mesh complexity and pixel resolution

Porcelain (12 images)	20 000 triangles	8 000 triangles	3 000 triangles
8.0M pixels	216 s	130 s	86s
3.2M pixels	162 s	112 s	96s
1.8M pixels	132 s	109 s	94s

The experimental results show that our provide solution work well with mesh complexity. Currently the majority of the computation time is spent on the blending of the texture to remove the artifacts.

We also compared the performance with the proposed weighted blending algorithm, Table 2 illustrates that the proposed method is not more efficient implementation compared with the "Best view" method, which due to the MRF optimization cost most of the time to smooth the borders of the texture patches.

Table 2 Comparison of the performance for different methods

	Buddha	Porcelain	Pottery	Jade ware
Triangles	4 600	4 000	6 000	3 500
Output textured resolution (in pixels)	3.2 M	2.1 M	1.8 M	1.3 M
MRF performance	82s	68 s	52 s	46 s
"Best view"performance	64 s	56 s	3 s	8 s

5 Conclusion

In this paper, we address the problem of creation of photorealistic 3D model using a dedicated optical digitizer, which is based on a m-FPP. The optical digitizer based on m-FPP is composed of a digital color camera, a B/W camera, and a DMD projector as basic units. To create a photorealistic model of real object, we suggested a seamless texture stitching approach that combines the MRF fragments mosaic optimization, and followed with a local compensation to remove the small miss-alignment introduce by the several phases, enhance the details of the final results. Experimental results validate the proposed approach and show that high quality and high resolution photorealistic model of 3D objects can be obtained. For future work, we shall consider how to make use of more information contained in captured images, which may be taken in diversified situations such as different lighting conditions. In that case, the properties such as the bidirectional reflectance distribution functions may be estimated to adapt to the environment in a real life.

References

[1] SMER E, TURKER M. Automatic near-photorealistic 3-D modelling and texture mapping for rectilinear buildings[J]. *Geocarto International*, 2016,215-223.

[2] JOHNSON R M, BRYSON M, DOUILLARD B, *et al*. Discovering salient regions on 3D photo-textured maps: Crowdsourcing interaction data from multitouch smartphones and tablets [J]. *Computer Vision and Image Understanding*, 2015, **131**: 28-41.

[3] AIGERMAN N, PORANNE R, LIPMAN Y. seamless surface mappings[J]. *ACM Transactions on Graphics*, 2015, **34**(4): 72:1-13.

[4] GENG J. Structured-light 3D surface imaging: a tutorial[J]. *Advances in Optics and Photonics*, 2011, **3**(2): 128-160.

[5] XU J, GAO B T, HAN J H, *et al*. Realtime 3D profile measurement by using the composite pattern based on the binary stripe pattern[J]. *Optics & Laser Technology*, 2012, **44**(3): 587-593.

[6] CHEN J, WU X J, YU W M, *et al*. 3D shape modeling using a self-developed hand-held 3D laser scanner and an efficient HT-ICP point cloud registration algorithm[J]. *Optics & Laser Technology*, 2013, **45**: 414-423.

[7] LIU X M, PENG X, YIN Y K, *et al*. Generation of photorealistic 3D image using optical digitizer[J]. *Applied Optics*, 2012, **51**(9): 1304-1311.

[8] LUDWIG M , BERRIER S , TETZLAFF M, *et al*. 3D shape and texture morphing using 2D projection and reconstruction[J]. *Comput Graph*, 2015, **51**: 146-156.

[9] ZHENG Shun-yi, ZHOU Yang. High quality reconstrution for small objects based on structure light scanning system with digital camera[J]. *Geomatics and Information Science of Wuhan University*, 2012,**37**(5): 529-533.

[10] LI A M, PENG X, YIN Y K,*et al*. Optical 3D digitizer for photorealistic imaging of movable cultural heritage[J]. *Acta Photonica Sinica*, 2013, **42**(12): 1421-1429.

[11] RODOLA E, ALBARELLI A, CREMERS D, *et al*. A simple and effective relevance-based point sampling for 3D Shapes[J]. *Pattern Recognition Letters*, 2015, **59**(1): 41-47.

[12] KARASZEWSKI M, SITNIK R, BUNSCH E. On-line, collision-free positioning of a scanner during fully automated three-dimensional measurement of cultural heritage objects[J]. *Robotics and Autonomous Systems* 2012, **60**(9): 1205-1219.

[13] ELFARARGY M, RIZQ A, RASHWAN M. 3D surface reconstruction using polynomial texture mapping[M]. Advances in Visual Computing: Springer Berlin Heidelberg,2013: 353-362.

[14] GOLDLUECKE B, CREMERS D. Superresolution texture maps for multiview reconstruction[C]. IEEE 12th International Conference on Computer Vision, Kyoto, Japan; 2009:1677-1684.

[15] GAL R, WEXLER Y, OFEK E, *et al*. Seamless montage for texturing models[C]. Comput Graph Forum, 2010: 479-486.

[16] ZHANG Z H, TOWERS C E, TOWERS D P. Time efficient color fringe projection system for 3D shape and color using optimum 3-frequency selection[J]. *Optical Express*, 2006, **14**(14): 6444-6455.

[17] PENG X, YIN Yong-kai, LIU Xiao-li. Phase-aided three-dimensional imaging and metrology[J]. *Acta Optica Sinica*, 2011, **31**(9): 0900120.

[18] ZHANG Z Y. A flexible new technique for camera calibration [J]. *IEEE Trans Pattern Anal Mach Intell* 2000, **22**(11): 1330-1334.

[19] BERNARDINI F, RUSHMEIER H, MARTIN I M, *et al*. Building a digital model of Michelangelo's Florentine Pieta [J]. *IEEE Comput Graph*, 2002, **22**(1): 59-67.

[20] BESL P J, MCKAY H D. A method for registration of 3-D shapes[J]. *IEEE T Pattern Anal*, 1992, **14**(2): 239-256.